International Journal of Thermal Sciences 87 (2015) 199–206

Contents lists available at ScienceDirect

International Journal of Thermal Sciences

journal homepage: www.elsevier.com/locate/ijts

Enhancement of laminar convective heat transfer relying on excitation of transverse secondary swirl flow

Jian Guo [a], Yuexiang Yan [b], Wei Liu [b], Fangming Jiang [a, *], Aiwu Fan [b, **]

[a] Laboratory of Advanced Energy Systems, CAS Key Laboratory of Renewable Energy, Guangzhou Institute of Energy Conversion, Chinese Academy of Sciences (CAS), Guangzhou 510640, China
[b] School of Energy and Power Engineering, Huazhong University of Science and Technology, Wuhan 430074, China

ARTICLE INFO

Article history:
Received 29 March 2014
Received in revised form
26 August 2014
Accepted 27 August 2014
Available online 26 September 2014

Keywords:
Convective heat transfer enhancement
Variation calculus
Laminar flow
Secondary swirl flow
Tube flow

ABSTRACT

Laminar forced convective heat transfer is studied for the purpose of getting the best heat transfer performance with the least flow resistance increase. The variation calculus method is employed to establish the equations describing the optimized fluid velocity field and temperature field. Numerical solutions of the equations for a convective heat transfer process in a section-cut of a square duct indicate the optimized flow should have a transverse secondary swirl flow pattern consisting of multiple vortexes with identical swirl direction in the junction region of any two neighboring vortexes. We then propose the convective heat transfer enhancement method relying on excitation of transverse secondary swirl flow. To validate this method, we numerically study the heat transfer and flow resistance characteristics of laminar flows in tubes with four-reverse-vortex-generator (FRVG) inserts, four-homodromous-vortex-generator (FHVG) inserts, or a twisted tape insert. The calculated transverse secondary flow in the tube with the FRVG inserts approximately follows the optimized flow pattern and the tube is thus found to have the best thermo-hydraulic performance, validating the proposed convective heat transfer enhancement method.

1. Introduction

Various techniques of convective heat transfer enhancement are widely applied in many industrial fields for efficient energy generation, conversion, and utilization. During the past several decades, many researchers and engineers have expended great efforts to develop advanced convective heat transfer enhancement techniques [1,2] like heat transfer surface modifications, direct flow stirrers and indirect flow stirrers by external electric or magnetic fields, to name a few. Fundamentally, these techniques strengthen the convection/advection of fluid flow and reduce the thickness of thermal boundary layer. For instance, the vortex generators destroy the boundary layer by generating longitudinal vortex near the tube-wall region [3,4], and the twisted tape inserts arouse overall swirl flows and enhance the fluid advection between the near-wall and central regions [5–7]. Therefore, these techniques or measures augment heat transfer rate normally at the cost of increasing the flow resistance, i.e., consuming more external pump work. In other words, there exists an intrinsic contradiction between convective heat transfer enhancement and flow resistance reduction. In order to comprehensively evaluate the overall performance of various heat transfer enhancement techniques, Webb [8] proposed a performance evaluation criterion (PEC), in terms of which a larger heat transfer rate does not necessarily mean a better overall performance as enough attention must be paid to the flow resistance increase after the implementation of the technique. Designing convective heat transfer enhancement techniques with maximized heat transfer enhancement effect at the cost of minimized external pump work consumption is persistently a hot research subject in the thermal science and engineering and relevant fields.

Bejan [9,10] proposed the principle of minimum entropy production for heat transfer optimization based on the idea that the entropy production in an optimized heat transfer process should be minimized. He derived the expression of entropy generation induced by both the heat transfer and viscous fluid flow and analyzed the optimum geometry of heat transfer enhancement devices at the constraint of least total entropy generation. Many researchers [11–17] analyzed the entropy generations in various

* Corresponding author. 2 Nengyuan Rd, Wushan, Tianhe District, Guangzhou 510640, China. Tel./fax: +86 20 87057656.
** Corresponding author. Tel.: +86 27 87542618; fax: +86 27 87540724.
E-mail addresses: fm_jiang2000@yahoo.com, fm_jiang2013@yahoo.com, jiangfm@ms.giec.ac.cn (F. Jiang), faw@mail.hust.edu.cn (A. Fan).

http://dx.doi.org/10.1016/j.ijthermalsci.2014.08.023
1290-0729/

convective heat transfer processes and found optimum geometrical parameters of relevant devices based on the principle of entropy production minimization. Relatively recently, some other objective functions for heat transfer optimization have been proposed, such as the entransy dissipation extreme by Guo et al. [18] and the power consumption minimization by Liu et al. [19,20]. Guo et al. [18] proposed a new concept, "entransy", and regarded it as a physical quantity describing the heat transfer ability and the potential capacity of a usable heat source. The fundamentals of their entransy theory are i) there is some inevitable entransy dissipation during heat transfer process, and ii) the entransy dissipation should be maximized or minimized for the optimization of a heat transfer process. Meng et al. [21] and Chen et al. [22] analyzed the entransy dissipation in some typical convective heat transfer processes and derived the expressions for process optimization. In contrast, Liu et al. [19,20] set the minimum power consumption as the optimization objective constrained by constant entransy dissipation and derived the modified expressions for the optimization of convective heat transfer in circular tube flows. In these works [18–22], the calculus of variations [23–25] was employed for the theoretical derivations.

Despite the aforementioned principles for heat transfer optimization, theories for the design of advanced convective heat transfer enhancement techniques are obviously still needed. This work is aimed to explore the mechanisms of convective heat transfer enhancement for laminar flows and attempts to develop a generic approach that can maximize the convective heat flux at the constraint of constant pump work consumption. We will first identify the objective function of heat transfer enhancement and the constraint function of pump work consumption. We then derive the equations that describe the optimized convective heat transfer in laminar flows based on the principle of the calculus of variations and apply these equations to a special case, convective heat transfer in a 2D section-cut of a square duct. Last, based on the findings from the results of 2D calculations, we propose a novel convective heat transfer enhancement method relying on excitation of transverse secondary swirl flow and numerically examine its effectiveness with respect to 3D tube flows.

2. Derivation of optimization equations

2.1. Heat transfer enhancement

To facilitate the derivation of equations, we consider a one-dimensional (1D) steady-state heat transfer process, schematic of which is depicted in Fig. 1. The left domain A is solid and the right domain B is fluid. The symbols n and T denote the 1D spatial position and the temperature variable, respectively. A constant temperature T_w is prescribed at the left boundary of domain A; T_w is higher than the temperature in the other regions. The heat is transported from the left boundary of domain A, across domain A by conduction, and into the fluid by convection. Besides maneuvering thermal properties of the solid or fluid, one more important way to enhance this heat transfer process is optimizing the velocity and temperature fields in the fluid domain B to enhance the heat convection.

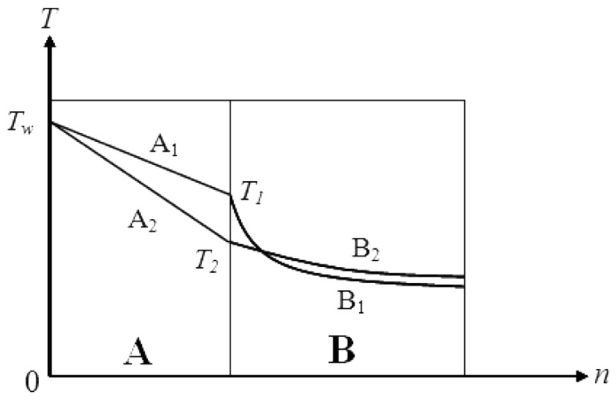

Fig. 1. Schematic of a one-dimensional heat transfer process.

The two temperature profiles (labeled with profile B_1 and B_2, respectively) are different due to the distinct velocity fields in domain B. Profile B_1 exhibits larger temperature gradients in the boundary layer, meaning that the heat transfer from the right boundary of domain A to the fluid is more inefficient. In contrast, profile B_2 is flatter, indicating more efficient heat transport. The temperature at the interface between the solid and fluid domains for profile B_2 is lower than that for profile B_1, i.e., $T_2 < T_1$. Since there is only heat conduction in the solid domain A, the temperature profiles A_1 and A_2, corresponding to B_1 and B_2 in the fluid domain, respectively, both show linear dependence on position n. Moreover, the temperature profile A_2 has larger gradients than profile A_1, indicating larger heat flux for scenario A_2. Therefore, the fluid flow in scenario A_2–B_2 has better effect of heat transfer enhancement than that in scenario A_1–B_1.

We turn the above discussion into the following mathematical expression, as

$$\left(\int_n |\partial T/\partial n|\mathrm{d}n\right)_2 < \left(\int_n |\partial T/\partial n|\mathrm{d}n\right)_1 \tag{1}$$

where the subscripts 1 and 2 denote profile B_1 and B_2, respectively, and the integrals over n are only on the fluid domain. The integral $\int|\partial T/\partial n|\mathrm{d}n$ quantifies the convective heat transfer enhancement effect for a fluid flow, and the smaller the value is the greater the effect can be. For two- or three-dimensional heat transfer processes, a generic expression is introduced as

$$J = \int_{\Omega} |\nabla T|\mathrm{d}\Omega \tag{2}$$

where, Ω represents the whole fluid domain. The smaller the J is the greater is the effect of convective heat transfer enhancement. Therefore, to enhance convective heat transfer, an effective method is to reduce the absolute value of temperature gradient in the fluid domain by manipulating the velocity distribution in the fluid.

Of course, all heat transfer processes must follow the energy conservation law, which is described by the following Eq. (3) if transient effects and energy sources/sinks are not considered.

$$k\nabla^2 T - \rho c_p \mathbf{U}\cdot\nabla T = 0 \tag{3}$$

2.2. External pump work consumption

External pump work is needed for forced convective heat transfer. When the convective heat transfer is enhanced by manipulating fluid velocity field, the external pump work consumption is inevitably increased for real viscous flow. The momentum equation of fluid flow describes the relationship between the forces and the fluid motions. We may identify the pump work consumption of viscous flow by comparing the momentum equations for viscous and inviscid flows.

For steady-state incompressible laminar flows, the momentum equations for inviscid and viscous flows, respectively, are

$$\rho\mathbf{U}\cdot\nabla\mathbf{U} = \boldsymbol{F} - \nabla p \tag{4}$$

$$\rho\mathbf{U}\cdot\nabla\mathbf{U} - \mu\nabla^2\mathbf{U} = \boldsymbol{F} - \nabla p \tag{5}$$

For inviscid flow, the imposed external forces ($\boldsymbol{F} - \nabla p$) can be totally contributed to the motions ($\rho\mathbf{U}\cdot\nabla\mathbf{U}$) of fluid; an external pump work is generally not needed. In contrast, an external pump work is a must for the viscous flow as the fluid flow needs to overcome the viscous resistance ($\mu\nabla^2\mathbf{U}$); the external force ($\boldsymbol{F} - \nabla p$) is not fully utilized to drive the motions ($\rho\mathbf{U}\cdot\nabla\mathbf{U}$) of fluid. Accordingly, the external pump work consumption for viscous flow is identified as

$$\text{consumption} = \int_{\Omega}\left(\mu\mathbf{U}\cdot\nabla^2\mathbf{U}\right)\mathrm{d}\Omega \tag{6}$$

where, the integral means the overall consumption across the whole flow field. Then the constraint of constant pump work consumption yields

$$\int_{\Omega}\left(\mu\mathbf{U}\cdot\nabla^2\mathbf{U}\right)\mathrm{d}\Omega = \psi \tag{7}$$

with ψ being a given constant.

2.3. Optimization equations

To optimize a convective heat transfer process, the value of the objective function J expressed by Eq. (2) should be minimized using the constraint expressed by Eq. (7), and this can be achieved via the calculus of variations. To facilitate the operations, we replace the objective function $\int_{\Omega}|\nabla T|\mathrm{d}\Omega$ with $\int_{\Omega}(\nabla T)^2\mathrm{d}\Omega$. In addition, the continuity equation is naturally one other constraint condition besides the energy equation (i.e., Eq. (3)) and the expression for constant pump work consumption (i.e., Eq. (7)). The continuity equation is expressed as

$$\nabla\cdot\mathbf{U} = 0 \tag{8}$$

Therefore, the Lagrange function for variation calculus is established as

$$J^* = \int_{\Omega}\left[(\nabla T)^2 + A\left(k\nabla^2 T - \rho c_p\mathbf{U}\cdot\nabla T\right) + B\nabla\cdot\mathbf{U} + C\left(\mu\mathbf{U}\cdot\nabla^2\mathbf{U}\right)\right]\mathrm{d}\Omega \tag{9}$$

where A, B and C are Lagrange multipliers. Both A and B are functions of spatial position, while C is required to be constant. Then the following Eqs. (10) and (12) can be derived from the variations of J^* with respect to T and $\mathbf{U}$,

$$k\nabla^2 A + \rho c_p\mathbf{U}\cdot\nabla A - 2\nabla^2 T = 0 \tag{10}$$

$$\int_{\Gamma}\left[(2\nabla T - \rho c_p A\mathbf{U} - k\nabla A)\delta T + kA\delta\nabla T\right]\mathrm{d}\vec{\Gamma} = 0 \tag{11}$$

$$2C\mu\nabla^2\mathbf{U} - \rho c_p A\nabla T - \nabla B = 0 \tag{12}$$

$$\int_{\Gamma}(B\delta\mathbf{U} - C\mu\mathbf{U}\cdot\nabla\delta\mathbf{U} + C\mu\delta\mathbf{U}\cdot\nabla\mathbf{U})\mathrm{d}\vec{\Gamma} = 0 \tag{13}$$

where, Γ represents the boundary face of the fluid domain and Eqs. (11) and (13) describe the general boundary conditions for Eqs. (10) and (12), respectively.

The equation group consists of Eqs. (3), (7), (8), (10) and (12) is closed for the solution of the variables A, B, C, $\mathbf{U}$ and T provided appropriate boundary conditions are given. The calculated velocity and temperature fields, which can have optimized heat transfer performance at the constraint of a given pump work consumption, may enlighten the design of advanced convective heat transfer enhancement techniques.

3. Excitation of transverse secondary flow

Normally, we solve Eqs. (3), (8), (10) and (12) to obtain the solutions of A, B, $\mathbf{U}$ and T, and then substitute the solution of $\mathbf{U}$ into Eq. (7) to derive the value of the constant C. It is obvious that the two constants, C and ψ, are related with each other, the smaller the former is the larger the latter can be. Accordingly, the constraint of constant pump work consumption is naturally sufficed by giving the value of the constant C. In this way, Eq. (7) is excluded during the solution procedure.

To clarify the concept more concisely, we consider only a convective heat transfer process in a 2D section-cut of a square duct. As depicted in Fig. 2, the length of each side of the square duct is 0.1 m; Dirichlet boundaries with constant temperatures $T_L = 300$ K and $T_R = 310$ K, are assumed for the left and right boundaries, respectively, and the other two boundaries are adiabatic walls. No-slip flow conditions are assumed for all the four boundary walls. Instead of using boundary conditions described by Eqs. (11) and (13), a special case of $A = 0$ is assumed for the left and right boundaries, and $\nabla A = 0$ for the other two boundaries; $B = 0$ is assumed for all the four boundaries. Heat is transferred from the left and right boundaries into the fluid region by the convection of airflow in the duct. To avoid flow vortexes caused by natural buoyancy forces, physical properties of the fluid are assumed constant as, $k = 2.59 \times 10^{-2}$ W m^{-1} K^{-1}, $\rho = 1.205$ kg m^{-3}, $\mu = 1.789 \times 10^{-5}$ Pa s, and $c_p = 1005$ J kg^{-1} K^{-1}. Cases of $C = 0.5$, 0.02 and 0.01 are specially selected for investigation.

The 2D square geometry was discretized using fine meshes, 100×100 quadrilateral meshes, which is sufficient to give results of satisfyingly high accuracy. In the present work, the commercial multi-functional CFD software package, FLUENT® 6.3 is employed to solve the Eqs. (3), (8), (10) and (12). Equation (3) is actually the steady-state energy conservation equation without any sources/sinks; Eq. (8) is the standard steady-state continuity equation for incompressible flow; Eq. (12) is similar to the steady-state momentum equation (i.e., Navier–Stokes equation) if we view the B as

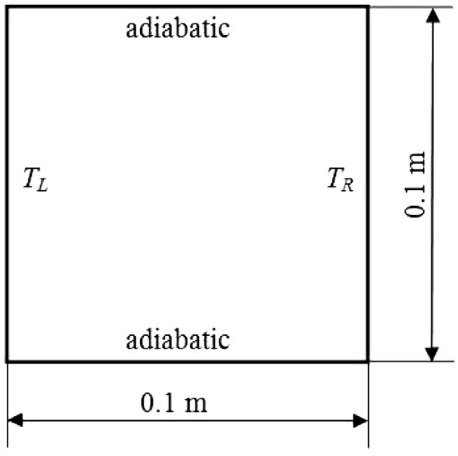

Fig. 2. Two-dimensional convective heat transfer process on a cross-sectional plane of a square duct.

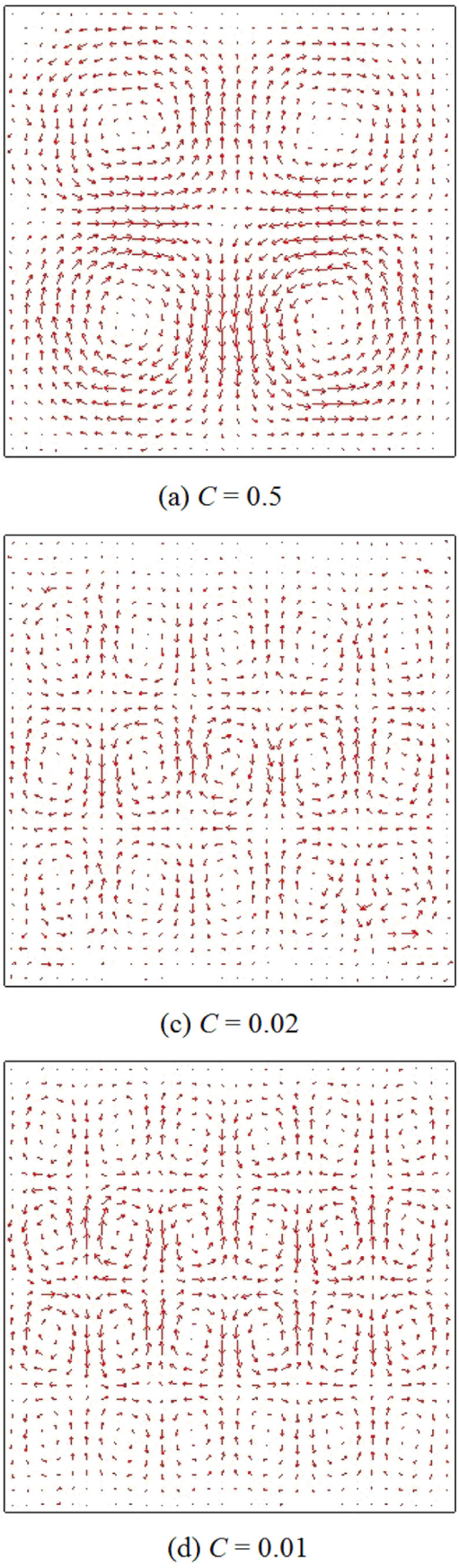

Fig. 3. Multi-vortex flow pattern forming on the 2D square plane. (Arrows in different plots are not drawn to scale to better view the flow pattern.)

the pressure variable in the N–S equation, but this momentum equation (Eq. (12)) has a non-standard viscous diffusion term and a non-standard source term. Equation (10) is a steady-state non-standard convective–advective equation for the variable A, and the first term on the right hand side of Eq. (10) is a diffusion term, the second a convective term, and the third a source term. We define a user defined scalar for the variable A and let the FLUENT itself solve the variables B, T and the vector $\mathbf{U}$ after customizing the non-standard terms and zero terms in Eqs. (3), (8), (10) and (12) with the FLUENT user defined functions (UDF). The SIMPLEC algorithm is used to resolve the coupling of the velocity vector and the variable B, and the QUICK discretization scheme is used to discretize the convection and diffusion terms.

Fig. 3 depicts the numerical results of velocity vectors for cases of different C values. Note that the vector arrows in different plots are not drawn to scale to better view the flow pattern. It is seen that the flow pattern of multiple vortexes emerges in the square for all the cases, and smaller C case shows more vortexes. The driving forces of these vortexes are from external pump work; for real cases, they can be generated, for instance, by an internal mechanical stirrer or an external electromagnetic device. According to the foregoing analyses, a smaller C means more consumption of pump work. Therefore, the multi-vortex flow pattern is related with the external pump work consumption: more pump work is consumed, more vortexes the resulting flow pattern has. It can be also found from Fig. 3 that the flow directions of adjacent vortexes are identical at the junctions. In the two-dimensional square, heat is convectively transferred between the walls and the fluid, which is similar to the convective heat transfer process on a section-cut of a three-dimensional duct flow. In this sense, the two-dimensional square can be looked as a section-cut of a three-dimensional square duct and the above-described vortexes can be viewed as the transverse secondary flow being added to the longitudinal main flow in three-dimensional square duct. This enlightens the invention of a novel convective heat transfer enhancement technique relying on the excitation of transverse secondary flow, which has at least two principles elaborated below.

First, the optimized velocity field has multiple vortex flow pattern on section-cut planes perpendicular to the main flow. This flow pattern is very different from that due to overall flow disturbance, a common mechanism of convective heat transfer enhancement for most of the current techniques, such as twisted tapes [5–7], coiled wires [26–28], conical strips [29–31] and porous media inserts [32,33]. Second, the fluid swirl directions are identical in the junction region of any two neighboring vortexes.

4. Validity tests

We consider tubes with specially designed inserts: the four-reverse-vortex-generator (FRVG) inserts, and the four-homodromous-vortex-generator (FHVG) inserts. As shown in Fig. 4(b) and (c), both the FRVG and FHVG inserts consist of a series of triangular sheets, geometry of which is sketched in Fig. 4(a). Each of the sheets is perpendicular to the horizontal plane but slants to the flow direction at an angle of $\alpha = 30^\circ$ and the lengths of its sides are $a = 0.005$ m and $b = 0.01$ m, respectively. The triangular sheet is very thin as compared with the side lengths, thereby its thickness is assumed to be 0. For the same group of four triangular sheets (FRVG or FHVG) the nearest distance (i.e., d) between two neighboring sheets is 0.005 m. Along the flow direction, multiple groups of FRVG inserts are aligned with a 0.04 m uniform pitch, i.e., $S = 0.04$ m. The diameter (D) and total length (L) of the tube are 0.025 m and 0.5 m, respectively. The dimensionless geometrical parameters of the FRVG inserts are determined as $a/D = 0.2$, $b/D = 0.4$, $d/D = 0.2$ and $S/D = 1.6$. In addition, a tube with a twisted tape insert as depicted

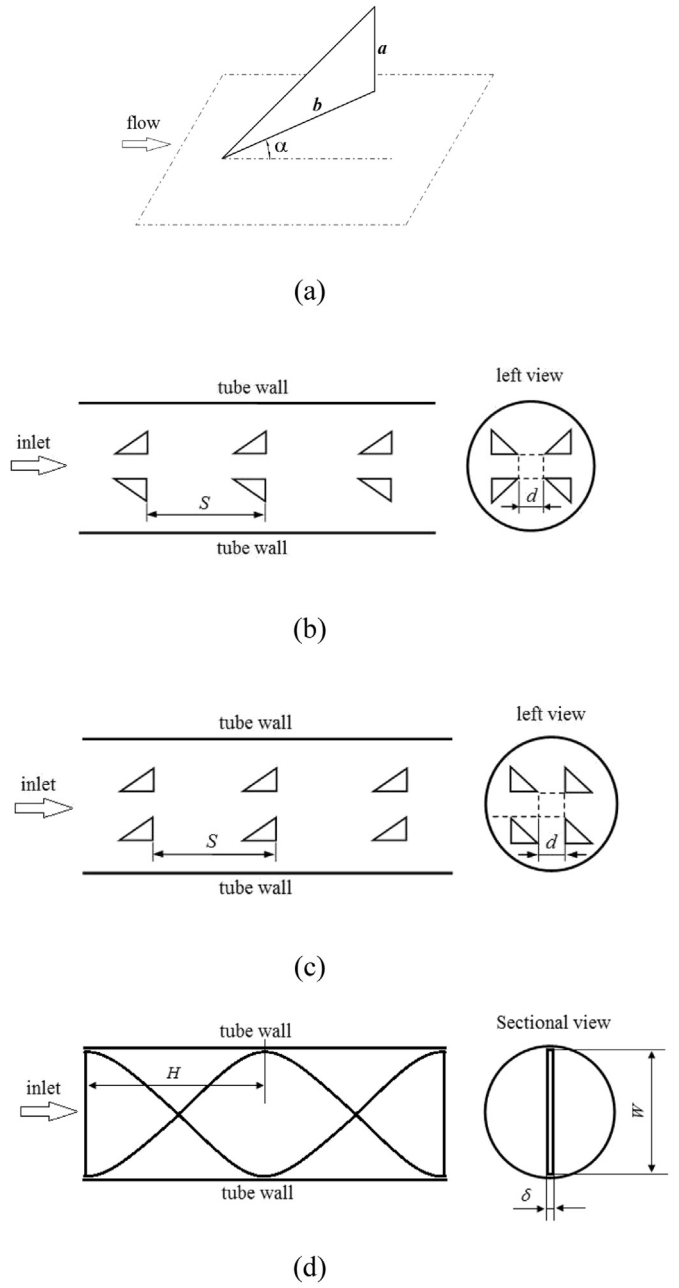

Fig. 4. (a) Geometry of the triangular sheet, (b) schematic of the tube with four-reverse-vortex-generator inserts, (c) schematic of the tube with four-homodromous-vortex-generator inserts, (d) schematic of the tube with a twisted tape insert.

in Fig. 4(d), which can be considered as a representative of a large class of heat transfer enhancement techniques relying on excitation of overall flow disturbance, is also taken into account mainly for comparison. The width (W) and thickness (δ) of the twisted tape are 0.025 m and 0.001 m respectively, and the twisted ratio (H/D) is 2.5; these parameters are specially designed to make it have the best heat transfer performance [5,6].

We employ FLUENT® 6.3 to simulate the convective heat transfer processes in the above-described three tubes. The working fluid is assumed to be air and its physical properties have already been detailed in Section 3. A constant heat flux is prescribed at the tube wall. To exclude the end-effects, at the tube inlet the fully developed velocity and temperature profiles for laminar flows, expressed by Eqs. (14) and (15) [34], respectively, are specified via FLUENT UDFs; at the outlet, a zero fluid pressure and zero heat flux boundary conditions are imposed. For the tube wall and the surfaces of inserts, no-slip wall boundaries are assumed.

$$u = u_c\left(1 - \frac{r^2}{R^2}\right) \tag{14}$$

$$T = T_c + \frac{qR}{k}\left[\left(\frac{r}{R}\right)^2 - \frac{1}{4}\left(\frac{r}{R}\right)^4\right] \tag{15}$$

where, u_c and T_c are the velocity and temperature at the center of the tube, respectively; q is the heat flux at the tube wall; R is the inner radius of the tube, and r is the radial distance to the center of the tube.

Grid-independence tests have been performed first. Tetrahedral numerical elements are used in meshing, and the meshes close to the tube wall and the surfaces of inserts are elaborately refined. Three mesh systems with ~1,100,000, 1,700,000 and 5,500,000 numerical elements, respectively, are adopted to calculate a baseline case of $Re = 1200$ for all the three tubes with FRVG inserts, FHVG inserts and a twisted tape insert, respectively. As explicit by Fig. 5, the calculated Nusselt number (Nu) and friction factor (f) values show small differences between the results based on the mesh systems of ~1,700,000 and 5,500,000 numerical elements, respectively. Moreover, inspection of the temperature and velocity data calculated from the two mesh systems with ~1,700,000 and 5,500,000 numerical elements, respectively, finds the differences are negligibly small. Therefore, the mesh system of ~1,700,000 numerical elements is adopted for all the following calculations.

Fig. 6 depicts the transverse secondary flow velocity vectors and contours on a tube sectional plane with a 0.25 m distance to the tube inlet for all the three tube flows. The Reynolds number (Re) for the flow is 1200. The secondary flow pattern shown in Fig. 6(a) is more similar to that shown in Fig. 3, which is an expected result owing to the FRVG inserts. Fig. 6(b) shows flow pattern different from Fig. 6(a); owing to the FHVG inserts, some of the forming vortexes exhibit reverse swirl direction in the junction region of two neighboring vortexes. Fig. 6(c) shows an overall disturbance to the tube flow by the twisted tape insert. It is noticeable from Fig. 6(a) that, besides the four major vortexes there are some additional minor vortexes forming in the gaps between the major vortexes. Similarly, some minor vortexes also appear for the tube with FHVG inserts, as seen in Fig. 6(b). All the vortexes, including the major and minor vortexes, displayed in Fig. 6(a), follow the two principles for the

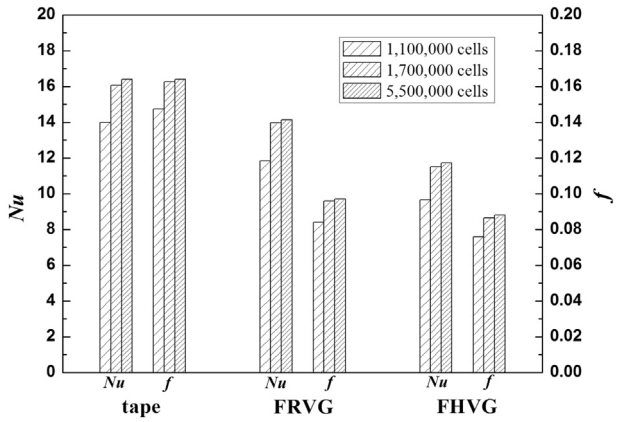

Fig. 5. Grid-independence tests: the calculated Nusselt number (Nu) and the friction factor (f) for tube flows with a twisted tape insert, FRVG inserts or FHVG inserts, based on numerical meshes of differing number of numerical elements.

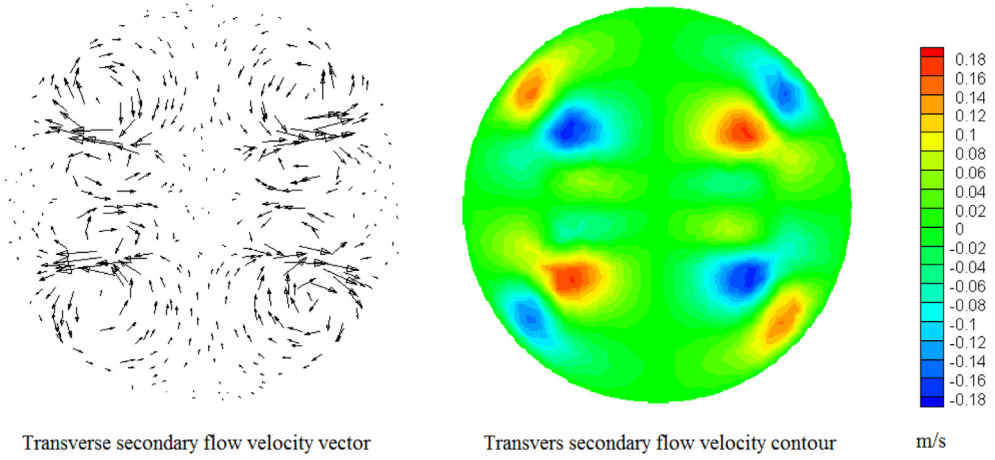

(a)

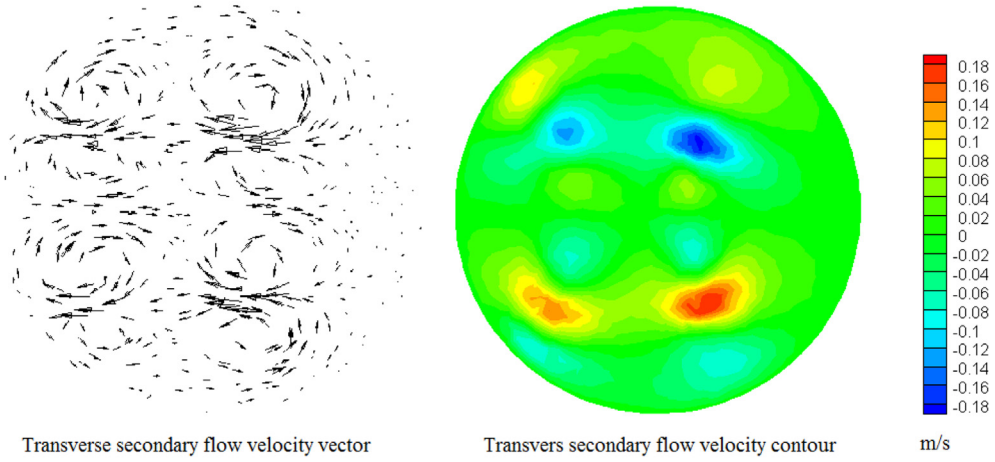

(b)

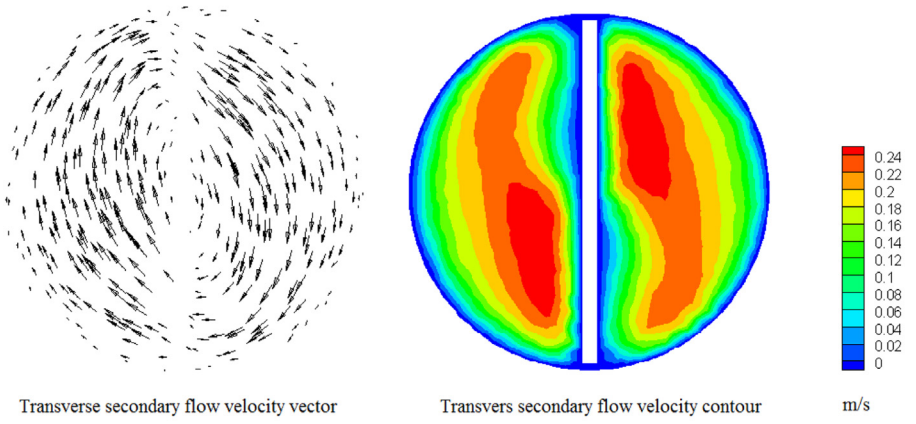

(c)

Fig. 6. Plots of transverse secondary flow velocity vectors and contours on a section-cut plane of the tube. *Re* = 1200 and (a) FRVG tube, (b) FHVG tube, and (c) tube with a twisted tape insert.

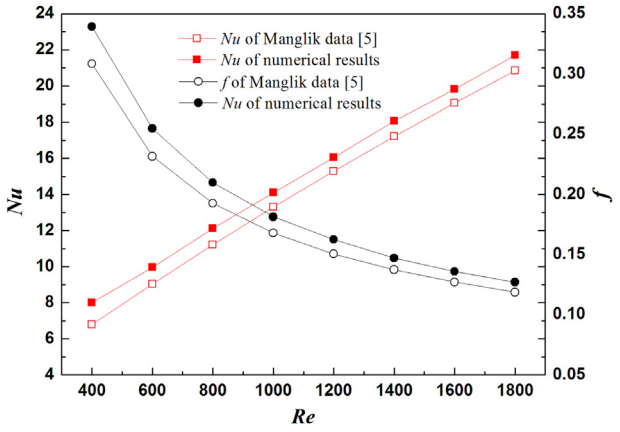

Fig. 7. Comparison of the numerical results and the experimental data for the tube with a twisted tape insert.

optimized secondary flow pattern described in Section 3. As some vortexes caused by the backflow of the major vortexes for the tube flows with FRVG or FHVG inserts, we see there exist regions with the secondary swirl flow of negative velocity magnitude.

Fig. 7 compares the numerical results and experimental data reported by Manglik [5] for the tube flow with a twisted tape insert. The calculated results deviate the experimental data by 3.8%–16.2% for *Nu* and 7.1%–9.4% for *f*.

The numerical results of the Nusselt number (*Nu*) and friction factor (*f*) for all the three tubes are summarized in Fig. 8. It can be seen that the tube of a twisted tape insert has the best heat transfer enhancement effect among the three, but the flow resistance increase is much larger than the other two; the tube flow with FRVG inserts has better heat transfer performance than that with FHVG inserts and the flow resistance of the former only shows some mild increase in comparison with the latter. To evaluate the overall thermo-hydraulic performance of these tubes, the performance evaluation criterion (PEC) proposed by Webb [8] is employed, which is defined as

$$\mathrm{PEC} = \frac{Nu/Nu_0}{(f/f_0)^{(1/3)}} \tag{16}$$

where, Nu_0 and f_0 are the Nusselt number and friction factor of the plain tube, respectively. In the present work, they are taken as $Nu_0 = 4.36$ and $f_0 = 64/Re$ for fully developed tube flow convective

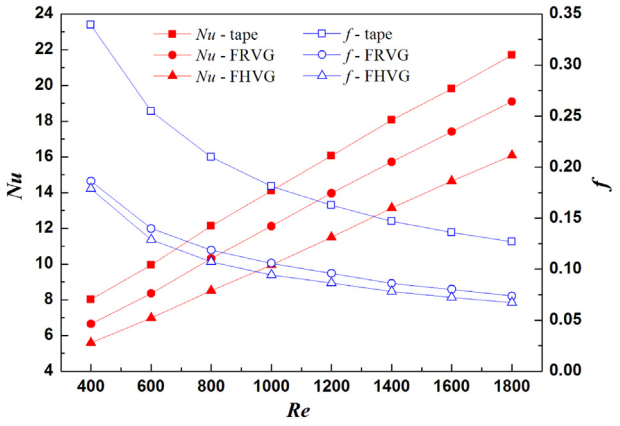

Fig. 8. The calculated Nusselt number (*Nu*) and friction factor (*f*) in the three tubes with FRVG inserts, FHVG inserts, and a twisted tape inserts, respectively.

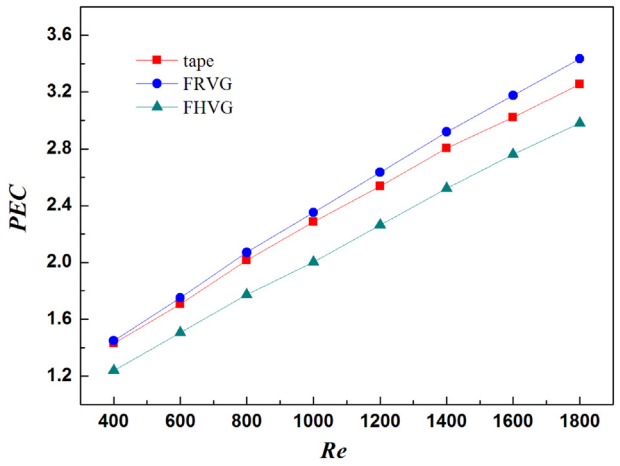

Fig. 9. Thermo-hydraulic performance (the calculated PEC values) for the three tubes with FRVG inserts, FHVG inserts, and a twisted tape insert, respectively.

heat transfer in laminar regime. Seen from Fig. 9, which compares the calculated PEC values for all the three tubes, the tube with the FRVG inserts has the largest PEC for the examined Reynolds numbers ranging from 0 to 1800, indicating the FRVG insert tube is the most advantageous heat transfer tube for laminar flows. The FHVG insert tube shows even worse heat transfer performance than the twisted tape insert tube, indicating the importance of arousing transverse vortexes with identical rotation directions in the junction region of neighboring vortexes for the proposed convective heat transfer enhancement technique.

5. Conclusion

Convective heat transfer for laminar flows has been studied theoretically in a generic way for the purpose of achieving maximum heat transfer enhancement effect at the constraint of constant pump work consumption. The objective function for heat transfer enhancement and the constraint function for external pump work consumption were derived, and the optimization equations for flow and temperature fields were established via the variation calculus method. The numerical solutions of the optimization equations showed that the optimized velocity field takes on a transverse secondary flow pattern of multiple vortexes with identical swirl direction at the junction of any two neighboring vortexes. Enlightened by these theoretical results, a novel convective heat transfer enhancement method for laminar flows was proposed, which relies on the excitation of transverse swirl flow. This secondary swirl flow consists of multiple vortexes and for a pair of neighboring vortexes the flow swirl directions are identical in the junction region. Specially, we realized this convective heat transfer enhancement concept in a tube with a group of FRVG inserts. Numerical results corroborated that the tube with FRVG inserts has superior overall heat transfer performance over the tubes with FHVG inserts or a twisted tape insert in laminar flow regime.

Acknowledgment

Financial support received from the China Natural Science Foundation (No.51036003), the Guangdong Natural Science Foundation (No.S2013040013967), the China National Key Basic Research Development Program (2013CB228302), and the CAS “100 Talents” Program (FJ) is gratefully acknowledged. The authors also indebtedly acknowledge the significant contribution to the scientific quality of this work made by the anonymous reviewers.

Nomenclature

A, B, C	Lagrange multipliers
a, b	length of the triangular sheet sides, m
c_p	specific heat at constant pressure, J kg^{-1} K^{-1}
D	diameter of the tube, m
d	distance of the triangular sheets, m
$\boldsymbol{F}$	volume forces
f	friction factor
H	180° twist pitch of the twisted tape, m
J	objective function
k	thermal conductivity, W m^{-1} K^{-1}
L	length of the tube, m
Nu	Nusselt number
n	one-dimensional space coordinate
p	pressure, N m^{-2}
q	heat flux density, W m^{-2}
R	inner radius of the tube, m
r	radial distance, m
Re	Reynolds number
S	pitch between the four-sheet elements, m
T	temperature, K
$\mathbf{U}$	flow velocity vector, m s^{-1}
u	flow velocity, m s^{-1}
W	width of the twisted tape, m

Greek symbols

α	slant angle (°)
Γ	boundary surface or line
δ	thickness of the twisted tape, m
μ	dynamic viscosity, m^2 s^{-1}
ρ	fluid density, kg m^{-3}
Ω	whole domain of the flow field
ψ	given value of power consumption

Subscripts

0	plain tube
c	centerline
L	left
R	right
w	tube wall

References

[1] A.E. Bergles, Handbook of Heat Transfer Applications, McGraw-Hill, New York, 1985.
[2] R.L. Webb, N.H. Kim, Principles of Enhanced Heat Transfer, second ed., Taylor & Francis Group, New York, 2005.
[3] P.A. Eibeck, J.K. Eaton, Heat transfer effects of a longitudinal vortex embedded in a turbulent boundary layer, J. Heat. Transf. 109 (1987) 17–24.
[4] W.R. Pauley, J.K. Eaton, The effect of embedded longitudinal vortex arrays on turbulent boundary layer heat transfer, J. Heat. Transf. 116 (1994) 871–878.
[5] R.M. Manglik, A.E. Bergles, Heat transfer and pressure drop correlations for twisted tape inserts in isothermal tubes: part I – laminar flows, ASME J. Heat. Transf. 115 (1993) 881–889.
[6] R.M. Manglik, A.E. Bergles, Heat transfer and pressure drop correlations for twisted tape inserts in isothermal tubes: part II – transition and turbulent flows, ASME J. Heat. Transf. 115 (1993) 890–896.
[7] J. Guo, A.W. Fan, X.Y. Zhang, W. Liu, A numerical study on heat transfer and friction factor characteristics of laminar flow in a circular tube fitted with center-cleared twisted tape, Int. J. Therm. Sci. 50 (2011) 1263–1270.
[8] R.L. Webb, Performance evaluation criteria for use of enhanced heat transfer surfaces in heat exchanger design, Int. J. Heat. Mass Transf. 24 (1981) 715–726.
[9] A. Bejan, Entropy Generation through Heat and Fluid Flow, Wiley, New York, 1982.
[10] A. Bejan, Entropy Generation Minimization, CRC Press, Florida, 1996.
[11] T.H. Ko, A numerical study on entropy generation and optimization for laminar forced convection in a rectangular curved duct with longitudinal ribs, Int. J. Therm. Sci. 45 (2006) 1113–1125.
[12] I. Dagtekin, H.F. Oztop, A.Z. Sahin, An analysis of entropy generation through a circular duct with different shaped longitudinal fins for laminar flow, Int. J. Heat. Mass Transf. 48 (2005) 171–181.
[13] A. Tandiroglu, Effect of flow geometry parameters on transient entropy generation for turbulent flow in circular tube with baffle inserts, Energy Convers. Manage. 48 (2007) 898–906.
[14] A. Arikoglu, I. Ozkol, G. Komurgoz, Effect of slip on entropy generation in a single rotating disk in MHD flow, Appl. Energy 85 (2008) 1225–1236.
[15] L. Zhao, L.H. Liu, Entropy generation analysis of electro-osmotic flow in open-end and closed-end micro-channels, Int. J. Therm. Sci. 49 (2010) 418–427.
[16] N. Sahiti, F. Krasniqi, X. Fejzullahu, J. Bunjaku, A. Muriqi, Entropy generation minimization of a double-pipe pin fin heat exchanger, Appl. Therm. Eng. 28 (2008) 2337–2344.
[17] T.A. Jankowski, Minimizing entropy generation in internal flows by adjusting the shape of the cross-section, Int. J. Heat. Mass Transf. 52 (2009) 3439–3445.
[18] Z.Y. Guo, H.Y. Zhu, X.G. Liang, Entransy—a physical quantity describing heat transfer ability, Int. J. Heat. Mass Transf. 50 (2007) 2545–2556.
[19] W. Liu, Z.C. Liu, H. Jia, A.W. Fan, A. Nakayama, Entransy expression of the second law of thermodynamics and its application to optimization in heat transfer process, Int. J. Heat. Mass Transf. 54 (2011) 3049–3059.
[20] H. Jia, W. Liu, Z.C. Liu, Enhancing convective heat transfer based on minimum power consumption principle, Chem. Eng. Sci. 69 (2012) 225–230.
[21] J.A. Meng, X.G. Liang, Z.X. Li, Field synergy optimization and enhanced heat transfer by multi-longitudinal vortexes flow in tube, Int. J. Heat. Mass Transf. 48 (2005) 3331–3337.
[22] Q. Chen, M. Wang, N. Pan, Z.Y. Guo, Optimization principles for convective heat transfer, Energy 34 (2009) 1199–1206.
[23] M.A. Biot, Variational principle in irreversible thermodynamics with applications to viscoelasticity, Phys. Rev. 97 (6) (1955) 1463–1469.
[24] B.A. Finlayson, L.E. Scriven, On the search for variational principles, Int. J. Heat. Mass Transf. 10 (1967) 799–821.
[25] B.A. Finlayson, The Method of Weighted Residuals and Variational Principles, with Application in Fluid Mechanics, Heat and Mass Transfer, Academic Press, New York, 1972.
[26] P. Promvonge, Thermal performance in circular tube fitted with coiled square wires, Energy Convers. Manage. 49 (2008) 980–987.
[27] A. Carcia, J.P. Solano, P.G. Vicente, A. Viedma, Enhancement of laminar and transitional flow in tubes by means of wire coil inserts, Int. J. Heat. Mass Transf. 50 (2007) 3176–3189.
[28] K. Yakut, B. Sahin, The effects of vortex characteristics on performance of coiled wire turbulators used for heat transfer augmentation, Appl. Therm. Eng. 24 (2004) 2427–2438.
[29] J. Guo, Y.X. Yan, W. Liu, F.M. Jiang, A.W. Fan, Effects of upwind area of tube inserts on heat transfer and flow resistance characteristics of turbulent flow, Exp. Therm. Fluid Sci. 48 (2013) 147–155.
[30] A.W. Fan, J.J. Deng, J. Guo, W. Liu, A numerical study on thermo-hydraulic characteristics of turbulent flow in a circular tube fitted with conical strip inserts, Appl. Therm. Eng. 31 (2011) 2819–2828.
[31] Y.H. You, A.W. Fan, W. Liu, S.Y. Huang, Thermo-hydraulic characteristics of laminar flow in an enhanced tube with conical strip inserts, Int. J. Therm. Sci. 61 (2012) 28–37.
[32] S.O. Akansu, Heat transfers and pressure drops for porous-ring turbulators in a circular pipe, Appl. Energy 83 (2006) 280–298.
[33] Z.F. Huang, A. Nakayama, K. Yang, C. Yang, W. Liu, Enhancing heat transfer in the core flow by using porous medium insert in a tube, Int. J. Heat. Mass Transf. 53 (2010) 1164–1174.
[34] J.P. Holman, Heat Transfer, ninth ed., McGraw–Hill, New York, 2002.